Identification of a Binding Domain of the Endothelin-B Receptor Using a Selective IRL-1620-Derived Photoprobe†

Stéphane Boivin,‡,§ Sophie Tessier,‡,§ Jacinthe Aubin,‡ Philipe Lampron,‡ Michel Detheux,|| and Alain Fournier*,‡

Institut National de la Recherche Scientifique−Institut Armand-Frappier, Université du Québec, 245 boul. Hymus, Pointe-Claire, Québec, Canada, H9R 1G6, and Euroscreen SA, 802 route de Lennik, 1070 Bruxelles, Belgium

Received April 15, 2004; Revised Manuscript Received June 25, 2004

ABSTRACT: On the basis of the structure of IRL-1620, a specific agonist of the endothelin-B receptor subtype (ET_B), a few photosensitive analogues were developed to investigate the binding domain of the receptor. Among those, a derivative containing the photoreactive amino acid, *p*-benzoyl-L-phenylalanine in position 5 showed, as assessed with endothelin-A (ET_A) and ET_B receptor paradigms, pharmacological properties very similar to those of IRL-1620. The binding capacity of the probe was also evaluated on transfected chinese hamster ovary (CHO) cells overexpressing the human ET_B receptor. Data showed that binding of the radiolabeled peptide was inhibited by ET-1 and IRL-1620. Therefore, this photolabile probe was used to label the ET_B receptor found in CHO cells. Photolabeling produced a ligand−protein complex appearing on SDS−PAGE at around 49 kDa. An excess of ET-1 or IRL-1620 completely abolished the formation of the complex, showing the selectivity of the photoprobe. Digestions of the [Bpa^5,$Tyr(^{125}I)^6$]IRL-1620−ET_B complex were carried out, and receptor fragments were analyzed to define the region of the receptor where the ligand interacts. Results showed that Endo Lys-C digestion gave a 3.8-kDa fragment corresponding to the Asp^{274}-Lys^{303} segment, whereas migration after V8 digestion revealed a fragment of 4.6 kDa. Because the fragments of these two digestions must overlap, the latter would be the Trp^{275}-Asp^{313} stretch. A cleavage with CNBr confirmed the identity of the binding domain by giving a fragment of 3.6 kDa, corresponding to Gln^{267}-Met^{296}. Thus, the combined cleavage data strongly suggested that the agonist binding domain of ET_B includes a portion of the fifth transmembrane domain, between residues Trp^{275} and Met^{296}.

Endothelin (ET)[1] is a potent vasoconstrictor peptide that was first isolated from the supernatant of cultured endothelial cells (*1*). Analysis of the ET gene revealed the existence of three distinct isoforms named ET-1, ET-2, and ET-3 (*2*). All those peptides include 21 residues and exhibit important sequence similarities; in particular, they all contain two intramolecular disulfide bonds in positions 1−15 and 3−11. As a potent vasoconstricting peptide hormone, ET can be an etiological factor of vascular diseases such as hypertension, heart failure, and local ischaemia, including myocardial infarction (*3*−*6*).

ET participates in the regulation of vascular tonus via two classes of cell-surface receptors designated as ET_A and ET_B (*7*). ET_A receptors are mostly located in vascular smooth muscle cells, where they play a major role in vasoconstriction, whereas ET_B receptors are predominantly found in vascular endothelial cells and induce vasodilatation through the production of nitric oxide. Nonetheless, ET_B receptors are also located on vascular smooth muscle cells and partly mediate their constriction (*8*).

ET receptors are members of the seven transmembrane (TM) super family of G protein-coupled receptors (GPCR), and their classification was initially established on the different activity and binding profiles obtained with the ET peptide isoforms. To date, a few studies were carried out to elucidate which segments of the ET receptors are crucial for ligand selectivity, activity, and affinity (*9*). For instance, site-directed mutagenesis showed that a large number of amino acids within ET_A, such as Gly^{97}, Lys^{140}, Lys^{159}, Gln^{165}, and Phe^{315} located respectively in TM regions 1, 2, 3, 3, and 6, influence ET-1 binding (*10*). Similarly, for ET_B, data from cross-linking experiments and chimeric ET_A/ET_B receptor studies concluded that a 60 amino acid domain spanning from

† Financial support was obtained from the Canadian Institutes for Health Research (CIHR). A.F. is "Chercheur National" from the Fonds de la Recherche en Santé du Québec (FRSQ). S.T. received a studentship from the Heart and Stroke Foundation of Canada (HSFC). S.B. and P.L. are recipients of a studentship from the Natural Sciences and Engineering Research Council of Canada (NSERC).

* To whom correspondence should be addressed. Telephone: (514) 630-8816. Fax: (514) 630-8850. E-mail: alain.fournier@inrs-iaf.uquebec.ca.

‡ Université du Québec.

§ Both authors contributed equally to the present study.

|| Euroscreen SA.

[1] Abbreviations: ACN, acetonitrile; Aebsf, 4-(2-aminoethyl)-benzenesulfonyl fluoride; Boc, *tert*-butyloxycarbonyl; BOP, benzotriazol-1-yl-oxy-tris(dimethylamino)-phosphonium hexafluorophosphate; Bpa, *p*-benzoyl-phenylalanine; BSA, bovine serum albumin; CHO, chinese hamster ovary; CNBr, cyanogen bromide; DIPEA, diisopropylethylamine; DMF, dimethylformamide; ECL, enhanced chemiluminescence; equiv, equivalent; ET, endothelin; ET_A and ET_B, endothelin type-A and -B receptors; GPCR, G protein-coupled receptor; HF, hydrofluoric acid; MALDI−TOF, matrix-assisted laser desorption ionisation−time-of-flight; PAGE, polyacrylamide gel electrophoresis; PVDF, polyvinylidene fluoride; SDS, sodium dodecyl sulfate; SEM, standard error of the mean; Suc, succinoyl; TFA, trifluoroacetic acid; TM, transmembrane.

10.1021/bi049246x CCC: $27.50
Published on Web 08/17/2004

Table 1: Amino Acid Sequence of IRL-1620 and Five Related Photoaffinity-Labeling Analogues

peptides	amino acid sequences
IRL-1620	Suc-Asp-Glu-Glu-Ala-Val-Tyr-Phe-Ala-His-Leu-Asp-Ile-Ile-Trp-COOH
[Bpa^4]IRL-1620	Suc-Asp-Glu-Glu-**Bpa**-Val-Tyr-Phe-Ala-His-Leu-Asp-Ile-Ile-Trp-COOH
[Bpa^5]IRL-1620	Suc-Asp-Glu-Glu-Ala-**Bpa**-Tyr-Phe-Ala-His-Leu-Asp-Ile-Ile-Trp-COOH
[Bpa^7]IRL-1620	Suc-Asp-Glu-Glu-Ala-Val-Tyr-**Bpa**-Ala-His-Leu-Asp-Ile-Ile-Trp-COOH
[Bpa^9]IRL-1620	Suc-Asp-Glu-Glu-Ala-Val-Tyr-Phe-Ala-**Bpa**-Leu-Asp-Ile-Ile-Trp-COOH
[Bpa^{10}]IRL-1620	Suc-Asp-Glu-Glu-Ala-Val-Tyr-Phe-Ala-His-**Bpa**-Asp-Ile-Ile-Trp-COOH

Ile^{138} to Ile^{197} (TM2−3) is the ET-1 binding site (*11*). In particular, an Asp residue highly conserved in TM2 of many GPCRs, corresponding to Asp^{147} in ET_B, was suggested as crucial, probably by participating to a hydrogen or electrostatic bond with the ligand or within the receptor itself. Such a phenomenon is frequent and, for instance, was described for the opioid receptors (*12*) as well as the natriuretic peptide receptors (*13*). However, another report produced after the evaluation of an Asp^{147}Ala−ET_B mutant showed that this modified receptor is devoid of any ability of activation, although ET-1 affinity was maintained, hence suggesting that Asp^{147} is rather required for receptor activation than ligand recognition (*14*). Another aspartic acid residue, conserved in many GPCRs and positioned in the TM3 region, was postulated to be involved in the binding of various ligands (*15*). Interestingly, lysine replaces this residue in the ET_B receptor (Lys^{182}), and its substitution using site-specific mutagenesis influenced the binding of ETs, without affecting G protein coupling (*16*). An additional lysine residue in ET_B, Lys^{161}, was also suggested to be important for ET high-affinity binding, because it may confer the nonselective binding characteristics of this receptor for ET isopeptides (*17*). In contrast, data published after the evaluation of a set of ET_B mutants are not in accordance with those results, because they rather demonstrate that binding determinants for ET_B selective agonists would be located in the TM4−6 and their adjacent loop regions (*18*). Moreover, Takasuka et al. showed that Asp^{75} and Pro^{93}, two residues found in the N-terminal extracellular domain, would be involved in the formation of a stable complex between the ET-1 ligand and its ET_B receptor (*19*).

All of these studies, mainly using site-directed mutagenesis, provided clues on some residues and their ability to modulate the ET_B receptor−ligand complex formation and activation. However, to further characterize the amino acids involved in these biological processes, other analytical methods must be explored. We then focused on photoaffinity labeling followed by fragmentation of the resulting photoligand−receptor complex for identifying sites of interaction between the ligand and the receptor. Benzoyl-phenylalanine (Bpa) (*20*), a photosensitive amino acid employed successfully to probe the substance P receptor (*21*), angiotensin II receptor (*22*), and urotensin II receptor (GPR14) (*23*) was exploited as a photolabile moiety.

In this paper, we describe the development of photoreactive probes exhibiting selectivity and agonistic activity toward the ET_B receptor. More precisely, a L-Bpa-scan approach of a synthetic linear analogue of ET-1, Suc-[Glu^9,Ala^{11,15}]-ET-1(8−21), specific to ET_B and known as IRL-1620 (*24*, *25*), was carried out to develop effective photolabile agonist ligands. In particular, the radioactive analogue [Bpa^5,Tyr-(^{125}I)^6]IRL-1620 exhibited the functional properties required for the covalent labeling of human ET_B receptors expressed in transfected chinese hamster ovary (CHO) cells. This step followed by the fragmentation of the photoligand−receptor complex enabled us to identify a binding domain interacting with the agonist photoprobe.

EXPERIMENTAL PROCEDURES

Materials. Male Sprague−Dawley rats and male Hartley guinea pigs were obtained from Charles River Canada (St-Constant, QC) and kept on a 12-h light−dark cycle with laboratory chow and tap water ad libitum according to standards approved by the Canadian Committee on Animal Care. Boc-L-Bpa was purchased from Advanced ChemTech (Louisville, KY). All other amino acids were obtained from ChemImpex International (Wood Dale, IL) or Albatross Chem Inc. (Montreal, QC). ; benzotriazol-1-yl-oxy-tris-(dimethylamino)-phosphonium hexafluorophosphate (BOP) was obtained from Albatross Chem Inc. (Montreal, QC). Chloramine-T, NaI, bovine serum albumin (BSA), protease inhibitor cocktail, succinic anhydride, CNBr, Endo Lys-C, V8 protease, and anti-ET_B receptor antibody were provided by Sigma−Aldrich (Oakville, ON). The Western blot ECL revelation kit, Na^{125}I and ^{14}C molecular weight standards were purchased from Amersham Biosciences (Montreal, QC). CHO cells stably expressing the human ET_B receptor were obtained from Euroscreen (Belgium). Ham-F12 culture medium, calf serum, and antibiotics were obtained from Biomedia (Drummondville, QC).

Photoprobes Synthesis. Probes were synthesized using a semiautomatic homemade solid-phase synthesizer, according to a protocol using *tert*-butyloxycarbonyl (Boc) chemistry. IRL-1620 (Suc-Asp-Glu-Glu-Ala-Val-Tyr-Phe-Ala-His-Leu-Asp-Ile-Ile-Trp) and five photosensitive analogues were synthesized by substituting successively Ala^4, Val^5, Phe^7, His^9, or Leu^{10} with a L-Bpa residue (Table 1). A chloromethylated resin was used as the solid support, and subsequent couplings of Boc amino acids (Boc-Asp(cHex)-OH, Boc-Glu(Bzl)-OH, Boc-Ala-OH, Boc-Val-OH, Boc-Tyr-(2BrZ)-OH, Boc-Phe-OH, Boc-His(Tos)-OH, Boc-Leu-OH, Boc-Ile-OH, and Boc-Trp(For)-OH) were performed in *N*,*N*-dimethylformamide (DMF) in the presence of diisopropylethylamine (DIEA) and BOP as a condensing reagent. L-Bpa was incorporated into peptides as a Boc-protected building block during solid-phase synthesis. The peptide resin was treated with succinic anhydride to obtain N^{α}-succinoylated derivatives. Peptide resins were cleaved with hydrofluoric acid (HF) (10 mL g^{-1}) using dimethyl sulfide and *m*-cresol as scavengers. The reaction was carried out for 1 h at 0 °C. HF was rapidly evaporated, and the resin was washed with diethyl ether. Crude synthetic peptides were extracted with TFA and precipitated with diethyl ether. Deformylation of the indole moiety of Trp^{14} was obtained by shaking the peptide (0.3 mg mL^{-1}) in 0.1 N piperidine at 0 °C for 15

min. Then, the solution was diluted with water (1:10), and peptides were purified by means of preparative reverse-phase HPLC using a Waters PrepLC500A system equipped with a model 441 absorbance detector and a Phenomenex Jupiter C_{18} (300 Å, 15 μm, 250 × 21.2 mm) column. Peptides were eluted with a linear gradient for 2 h from A (aqueous NH_4-OH at 0.05%) to B (20% ACN in solvent A). Flow rate was maintained at 20 mL min^{-1}, and detection was at 229 nm. Collected fractions were analyzed using reverse-phase HPLC. Fractions corresponding to pure material were pooled, lyophilized, and analyzed by mass spectrometry. Purification led to peptide purity equal to or greater than 98%, and their molecular mass was confirmed with MALDI−TOF mass spectrometry (Voyager-DE, PerSeptive Biosystems, Foster City, CA). Peptides in a powder form were kept at −20 °C until biological and biochemical characterizations.

Iodination with "Cold" Iodine. Peptides (40 mg) were dissolved in a Tris-HCl buffer (0.25 mM at pH 7.5) containing NaCl (0.05 M) and 1.5 equiv of NaI. Chloramine-T (0.8 equiv) was added to start the reaction. After 30 s, 2 equiv of sodium metabisulfite ($Na_2S_2O_5$) was added to stop the reaction. Then, the mono and diiodo forms of the peptides were isolated by preparative reverse-phase HPLC using a linear gradient (0−30% ACN/aqueous NH_4OH at 0.05%). Peptide purity was assessed with analytical reverse-phase HPLC, and molecular weight was determined using MALDI−TOF mass spectrometry.

Pharmacological Evaluations. The biological activity of the probes was assessed in two different preparations, rat thoracic aorta rings (*26*) and guinea pig lung parenchyma strips (*27*). Male Sprague−Dawley rats (250−300 g) were anesthetized, and the thoracic aorta was removed and cleaned of connective tissues, Its endothelium was detached by gentle rubbing. Rings (4-mm wide) were cut and mounted under an initial tension of 1 g, in water-jacketed organ baths containing oxygenated Krebs buffer (120 mM NaCl, 25 mM $NaHCO_3$, 11 mM glucose, 4.7 mM KCl, 2.4 mM $MgSO_4$, 1.17 mM KH_2PO_4, and 2.5 mM $CaCl_2$) maintained at 37 °C. Each preparation was allowed to equilibrate for 1 h, and contractions were recorded using a Grass 7E Polygraph equipped with force−displacement transducers. Contractile responses were measured for concentrations of peptides ranging from 10^{-10} to 10^{-5} M. The biological activity was expressed as a percentage of the effect produced by KCl (80 mM).

Male Hartley guinea pigs (300−350 g) were anesthetized, and lungs were removed. The parenchyma was dissected in strips that were mounted in the system described above. Contractile responses were measured for concentrations of peptides ranging from 10^{-10} to 10^{-5} M. The biological activity was expressed as a percentage of the effect produced with histamine (10^{-6} M). Noniodinated and iodinated peptides were tested, and concentration−response curves were analyzed using a nonlinear least-squares regression carried out with the Prism 3.02 software (GraphPad Software Inc., San Diego, CA). Results are expressed as mean ± SEM, and *n* varied from 8 to 12 animals.

Cell Culture. CHO cells stably expressing the human ET_B receptor were grown at 37 °C with 5% CO_2 in Ham F-12 nutriment medium supplemented with 10% fetal calf serum, 400 μg mL^{-1} of G418, 100 units mL^{-1} penicillin, 100 units mL^{-1} streptomycin, and 2.5 units mL^{-1} amphotericin B.

Immunoblotting. The molecular weight of the ET_B receptor was determined by an immunoblot analysis. Cells cultured in 100-mm dishes were solubilized in 1.5 mL of a detergent buffer (50 mM Tris-HCl at pH 7.4, 150 mM NaCl, 0.5% (v/v) Igepal, 0.1% (w/v) sodium dodecyl sulfate (SDS), 0.1% (v/v) Triton, 5 mM EDTA, and 0.01% (v/v) cocktail of inhibitors) and submitted to a gentle agitation at 4 °C. Then, the solution was centrifuged at 20000*g* for 45 min, and proteins of the supernatant were separated by 10% SDS−PAGE. Proteins were transferred to a PVDF membrane by electrophoretic blotting and probed with a polyclonal antibody against hET_B. Reactivity to the antibody was detected by chemiluminescence using an ECL Western blotting system and exposed to an X-ray film (Universal X-ray Company of Canada Ltd., Dorval, QC).

Radioiodination. Iodine-125 was incorporated into the tyrosine residue following a modified protocol described by Watakabe and co-workers (*25*). Briefly, the peptide (6.6 nmol) was dissolved in 13 μL of 100 mM sodium phosphate buffer (pH 7.5). Then, 1 mCi of $Na^{125}I$ (10 μL) was added, and the reaction was initiated with the addition of chloramine-T (14 nmol). The solution was mixed for 30 s, and the reaction was stopped by adding 100 μL of 10 mM sodium metabisulfite. The ^{125}I-labeled peptides were purified by analytical reverse-phase HPLC using a linear gradient of 30−60% ACN in aqueous TFA (0.06%), at a flow rate of 1 mL min^{-1}. Fractions were collected every 30 s, and the radioactivity was monitored with a Cobra II γ counter (Packard−Canberra, Montreal, QC). The monoradioiodinated peptides were diluted 1:10 in 100 mM sodium phosphate buffer (pH 7.5) and stored at −20 °C until their use. Specific activity was assumed to be at 2200 Ci/mmol.

Binding Studies. Binding assays were performed with CHO-ET_B cells cultured in 12-well culture plates until confluence was reached. The culture medium was aspirated, and cells were washed twice with cold buffer A (25 mM Tris-HCl, 5 mM $MgCl_2$, and 100 mM NaCl at pH 7.4). Competition binding experiments were performed in 0.5 mL of buffer A supplied with 0.01% (w/v) BSA and 0.01% (v/v) protease inhibitor cocktail containing AEBSF, aprotinin, leupeptin, bestatin, pepstatin A, and E-64. Cells were incubated for 16 h at 4 °C with monoradioiodinated peptides (3×10^{-10} M) in the presence of IRL-1620 or ET-1, at concentrations ranging from 10^{-12} up to 10^{-6} M. The incubation was terminated by rapid removal of the binding buffer, and cells were washed twice with cold buffer A. Cells were collected with a 1 M NaOH solution and transferred to a test tube to allow a radioactivity count. The extent of displacement (IC_{50}) was determined by a nonlinear regression according to a single-site model using the Prism 3.02 software. Results are expressed as the mean ± SEM of three independent determinations carried out in duplicate.

Photolabeling of ET_B Receptors. Transfected CHO-ET_B cells were incubated for 16 h at 4 °C with 6 nmol of radiophotoreactive analogue in buffer A supplied with 0.01% (v/v) protease inhibitor cocktail. Cells were washed, covered with 750 μL of the same buffer, and then irradiated with UV (with a 100 W lamp; 365 nm) at a distance of 6 cm, for 1 h, while kept on ice. Afterward, 750 μL of the detergent buffer was added and cells were submitted to a gentle agitation for 45 min. The solutions were then centrifuged at

16000*g* for 45 min at 4 °C. The supernatants were stored at −20 °C until further analysis.

Identification of the Labeled Complex. The solubilized photolabeled receptors were diluted 1:2 with a loading buffer (62.5 mM Tris-HCl at pH 6.8, 20% (v/v) glycerol, 2% (w/v) SDS, 5% (v/v) β-mercaptoethanol, and 0.025% (w/v) bromophenol blue) and incubated for 1 h at 37 °C. A 10% SDS−polyacrylamide gel electrophoresis (PAGE) was performed using a 1-mm-thick gel as described by Laemmli (*28*). After a migration of 175 V for 1 h, the gels were dried on filter paper and exposed to X-ray film with an intensifying screen. [^{14}C]Methylated molecular standards (14−220 kDa) were used to determine the molecular mass of the radiolabeled complex.

Partial Purification of the Photolabeled Complex. The solubilized photolabeled receptors were diluted 1:2 with the loading buffer described above and incubated for 1 h at 37 °C. A 10% SDS−PAGE electrophoresis was performed using a 1.5-mm-thick gel. The gel was then cut into slices, and their radioactive content was measured with a γ counter. The labeled receptor was electroeluted from the gel slices into electroelution buffer (25 mM Tris base, 192 mM glycine, and 0.1% SDS) for 3.5 h at room temperature as recommended by the electroelution apparatus protocol of the manufacturer (Bio-Rad, Mississauga, ON). The eluate was concentrated to a final volume of 30 μL using Centricon-10 and was stored at −20 °C.

Proteolytic and Chemical Digestion. For CNBr cleavage, the partially purified photolabeled receptor was resuspended in 200 μL of 50% (v/v) TFA/H_2O before adding 200 μL of ACN containing 50 mg of CNBr. The samples were incubated at room temperature in the dark for 16−18 h. The reaction was terminated by adding 3 mL of water. Samples were lyophylized twice to remove a large part of the salts. For proteolytic digestions, partially purified photolabeled receptors were digested for 16−20 h at 37 °C with 1 μg of Endo Lys-C protease in 25 μL of digestion buffer containing 25 mM Tris-HCl at pH 8, 1 mM EDTA, and 0.1% SDS. Partially purified receptors were also digested for 7 days at room temperature with 8 μg of V8 protease in 25 μL of buffer containing 100 mM ammonium carbonate at pH 8 and 0.1% SDS. All digestions were terminated by addition of an equal volume of Laemmli buffer followed by an incubation at 37 °C for 1 h.

Analysis of Products of Proteolysis and Chemical Cleavage. The products of proteolysis and chemical cleavage were analyzed by SDS−PAGE using 16.5% Tris-Tricine gels. After a migration of 80 V for 4 h, the gels were dried on filter paper and exposed to X-ray film with an intensifying screen. ^{14}C-Labeled low molecular protein standards (5−30 kDa) were used to determine the molecular mass of the photolabeled fragments.

RESULTS

Peptide Synthesis and Purification. Table 1 shows the amino acid sequences of the specific ET_B receptor agonist, IRL-1620, and five photosensitive analogues. The amino acids Ala^4, Val^5, Phe^7, His^9, and Leu^{10} were replaced successively with a L-Bpa residue. The photoprobes were assembled with the so-called Boc chemistry protocol, using BOP as the coupling reagent. Purity of the peptides (≥98%) was assessed by analytical HPLC. Mass spectrometry analysis using MALDI−TOF technology confirmed the exact mass of all synthetic compounds.

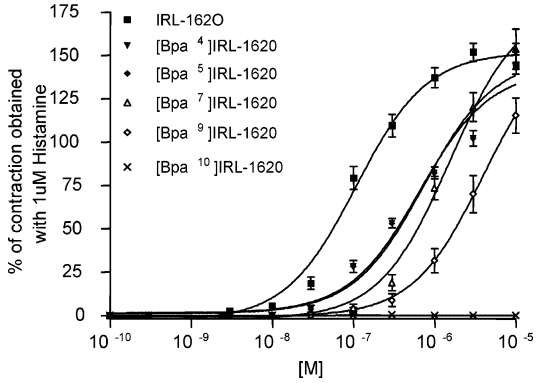

FIGURE 1: Concentration−response curves of IRL-1620 (■) and its photosensitive analogues [Bpa^4]IRL-1620 (▼), [Bpa^5]IRL-1620 (◆), [Bpa^7]IRL-1620 (△), [Bpa^9]IRL-1620 (◇), and [Bpa^{10}]IRL-1620 (×) obtained with the guinea-pig lung parenchyma strip bioassay (ET_B preparation). Results are expressed as a percentage of the contractile response induced with 10^{-6} M histamine.

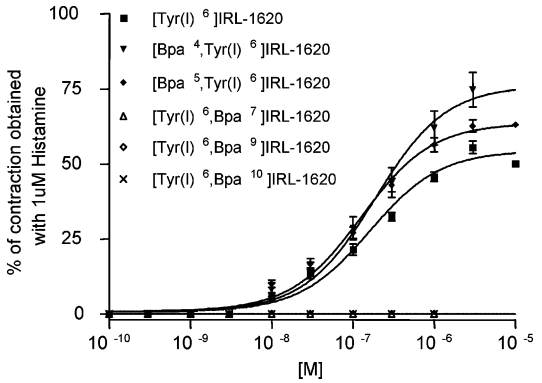

FIGURE 2: Concentration−response curves of [Tyr(I)^6]IRL-1620 (■) and the iodinated Bpa analogues [Bpa^4,Tyr(I)^6]IRL-1620 (▼), [Bpa^5,Tyr(I)^6]IRL-1620 (◆), [Tyr(I)^6,Bpa^7]IRL-1620 (△), [Tyr(I)^6,-Bpa^9]IRL-1620 (◇), and [Tyr(I)^6,Bpa^{10}]IRL-1620 (×) obtained in the guinea-pig lung parenchyma strip bioassay (ET_B preparation). Results are expressed as a percentage of the contractile response induced with 10^{-6} M histamine.

Activity Assays. The biological activity of the photoprobes was measured in the rat thoracic aorta and guinea pig lung parenchyma bioassays, two pharmacological preparations showing predominant populations of ET_A and ET_B receptors, respectively. Figures 1 and 2 show the concentration−response curves of the active compounds, and Table 2 summarizes the results. IRL-1620 at concentrations varying from 10^{-10} to 10^{-6} M induced concentration-dependent contractions in guinea pig lung parenchyma strips with an EC_{50} of 110 nM. The photoreactive analogues were however not as potent as IRL-1620, meaning that the amino acid residues Ala^4, Val^5, Phe^7, or His^9 of IRL-1620 exhibit variable tolerance toward a substitution with a bulky moiety such as Bpa. It is even more obvious with position 10 because the substitution of Leu^{10} with Bpa resulted in a complete loss of activity on ET_B receptors. Moreover, this analogue did not show any antagonistic properties in the ET_B preparation. None of the five peptides produced a biological effect, neither as agonist nor antagonist, in the rat thoracic aorta assay suggesting that the active probes were still highly selective for the ET_B receptor.

Table 2: Biological Activities of IRL-1620 and Photosensitive Analogues in the Rat Thoracic Aorta (ET_A) and Guinea-Pig Lung Parenchyma (ET_B) Bioassays

peptides	ET_A preparation $EC_{50} \pm$ SEM (M)	ET_B preparation $EC_{50} \pm$ SEM (M)
IRL-1620	na[a]	$1.1 \pm 0.9 \times 10^{-7}$
[Bpa^4]IRL-1620	na	$7.4 \pm 0.7 \times 10^{-7}$
[Bpa^5]IRL-1620	na	$6.5 \pm 0.6 \times 10^{-7}$
[Bpa^7]IRL-1620	na	$1.6 \pm 0.2 \times 10^{-6}$
[Bpa^9]IRL-1620	na	$>10^{-6}$
[Bpa^{10}]IRL-1620	na	na
[Tyr(I)^6]IRL-1620	na	$1.6 \pm 0.1 \times 10^{-7}$
[Bpa^4,Tyr(I)^6]IRL-1620	na	$1.9 \pm 0.2 \times 10^{-7}$
[Bpa^5,Tyr(I)^6]IRL-1620	na	$1.3 \pm 0.1 \times 10^{-7}$
[Tyr(I)^6,Bpa^7]IRL-1620	na	na
[Tyr(I)^6,Bpa^9]IRL-1620	na	na
[Tyr(I)^6,Bpa^{10}]IRL-1620	na	na

[a] na = not active.

Radioiodination of the probes is an essential step to subsequently allow the visualization of the photolabeled receptor. Hence, a second series of pharmacological activity was evaluated with the probes after iodination with "cold" iodine to confirm that the incorporation of this atom into the phenolic ring of Tyr^6 does not abolish the activity nor binding capacity of the IRL-1620 derivatives. So far, iodination of IRL-1620 led to a 50% decrease in efficacy, while the EC_{50} value did not appear to be influenced. On the other hand, as seen with [Bpa^4,Tyr(I)^6]IRL-1620, iodination of tyrosine gave rise to an improvement of the EC_{50} (740 ± 70 versus 190 ± 20 nM). A similar result was obtained with [Bpa^5,Tyr(I)^6]IRL-1620 in which iodination improved the EC_{50} by 5-fold (650 ± 60 versus 130 ± 10 nM). Despite their enhanced potencies, their contractile response was however 50% less effective in the ET_B receptor bioassay. Iodination of [Bpa^7]IRL-1620 and [Bpa^9]IRL-1620 completely abolished their activity and binding capacity on ET_B receptors, while [Tyr(I)^6,Bpa^{10}]IRL-1620 did not exhibit any activity nor binding capacity. All iodinated analogues were inactive in the rat thoracic aorta bioassay.

Binding Experiments. CHO cells expressing the human ET_B receptor (Figure 3) were used to assess the binding potencies of the photoprobes. Because no antagonistic effects were measured with the ET_B inactive analogues, only the compounds showing a biological activity on the ET_B receptor were evaluated on the CHO cells. Binding capacity assessment was carried out by competitive binding assays using [Bpa^4,Tyr(^{125}I)^6]IRL-1620 and [Bpa^5,Tyr(^{125}I)^6]IRL-1620 as tracers. As shown in Figure 4A, binding of [Bpa^5,Tyr(^{125}I)^6]-IRL-1620 was inhibited by ET-1 (IC_{50} value of 1.8 ± 0.3 nM) and IRL-1620 (IC_{50} value of 52 ± 1 nM). Similar results were obtained with the radioligand [Tyr(^{125}I)^6]IRL-1620 when using ET-1 as a competitor (IC_{50} value of 1.0 ± 0.1 nM) (Figure 4B). However, IRL-1620 (IC_{50} value of 2.3 ± 0.1 nM) exhibited a more pronounced ability to displace radioiodinated IRL-1620 than its Bpa^5 counterpart (Figure 4B). Although, [Bpa^4,Tyr(I)^6]IRL-1620 was an agonist as good as [Bpa^5,Tyr(I)^6]IRL-1620, its behavior as a tracer was unsatisfactory, and only a weak binding was observed with this peptide. Nevertheless, the binding experiments demonstrated that [Bpa^5,Tyr(^{125}I)^6]IRL-1620 is very well-recognized by ET_B receptors and shares the same binding site as ET-1. This photoprobe has then been favored for photoaffinity labeling.

Photoaffinity Labeling of ET_B Receptors. As shown with a 10% SDS−PAGE analysis, photoactivation of [Bpa^5,Tyr(^{125}I)^6]IRL-1620 bound to ET_B receptors found at the surface of CHO cells resulted in the covalent attachment of this probe (lane 1 of Figure 5A; 49-kDa complex and a minor component at 37 kDa). Interestingly, a previous treatment with PNGase F did not modify the separation pattern, thus suggesting that ET_B is not a glycoprotein (data not shown). The formation of the complex between [Bpa^5,Tyr(^{125}I)^6]IRL-1620 and the receptor was completely abolished in the presence of ET-1 (lane 2) or IRL-1620 (lane 3), demonstrating the specificity of the labeling. In addition, the identity of the ET_B receptor has been confirmed by immunoblotting experiments (Figure 5B), that showed that a 47-kDa protein

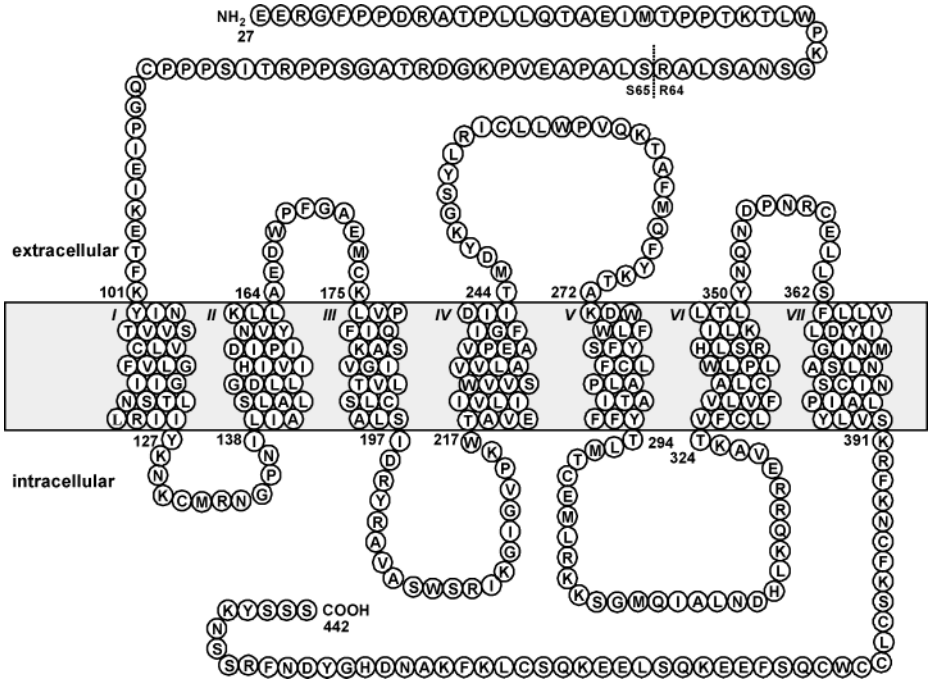

FIGURE 3: Primary structure of the human ET_B receptor.

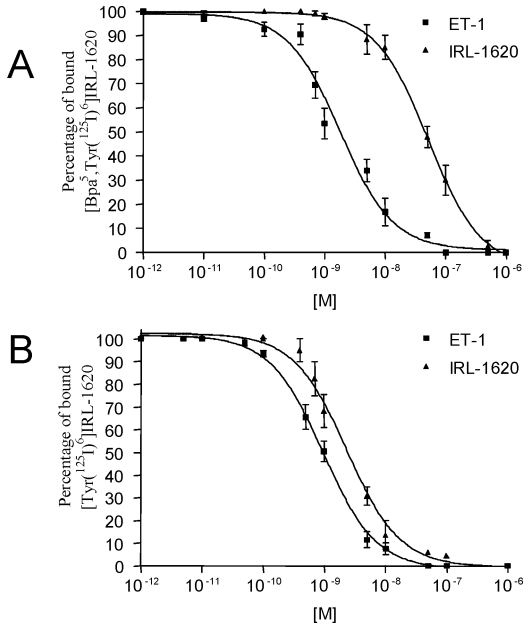

FIGURE 4: Competition binding curves of ET-1 (■) and IRL-1620 (▲) for the binding of [Bpa^5,$Tyr(^{125}I)^6$]IRL-1620 (A) or [$Tyr(^{125}I)^6$]-IRL-1620 (B) to ET_B receptors expressed in transfected CHO cells. The IC_{50} values for the displacement of [$Tyr(^{125}I)^6$]IRL-1620 binding to ET_B receptors for ET-1 and IRL-1620 are $1.0 \pm 0.1 \times 10^{-9}$ and $2.3 \pm 0.1 \times 10^{-9}$ M, respectively. The IC_{50} values for the displacement of [Bpa^5,$Tyr(^{125}I)^6$]IRL-1620 are $1.8 \pm 0.3 \times 10^{-9}$ M for ET-1 and $52 \pm 1 \times 10^{-9}$ M for IRL-1620. The data are shown as a percentage of the specific control binding determined in the absence of competing ligands and are representative of three to five similar independent experiments conducted in duplicate.

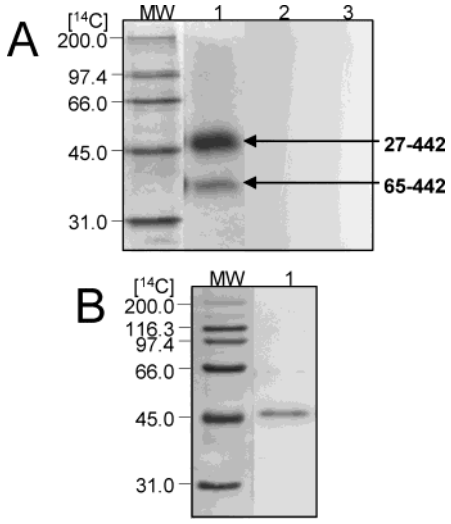

FIGURE 5: ET_B receptor analysis by SDS−PAGE. (A) Specific photolabeling of ET_B receptors with [Bpa^5,$Tyr(^{125}I)^6$]IRL-1620. CHO cells transfected with ET_B receptors were incubated with [Bpa^5,$Tyr(^{125}I)^6$]IRL-1620 either alone (lane 1), in the presence of 1 μM unlabeled ET-1 (lane 2), or in the presence of 1 μM unlabeled IRL-1620 (lane 3). (B) Immunoblot analysis of ET_B receptors. Protein standards of the indicated molecular masses (in kilodaltons) were run in parallel. These results are representative of at least three separate experiments.

is recognized by antibodies raised against the ET_B receptors. Thus, the 49-kDa photolabeled protein would be the mass of the photosensitive ligand (1972 Da) linked to the ET_B receptor (47 kDa). On the other hand, the 37-kDa photolabeled protein would be a proteolytic truncated form of the receptor appearing during the photolabeling process, because

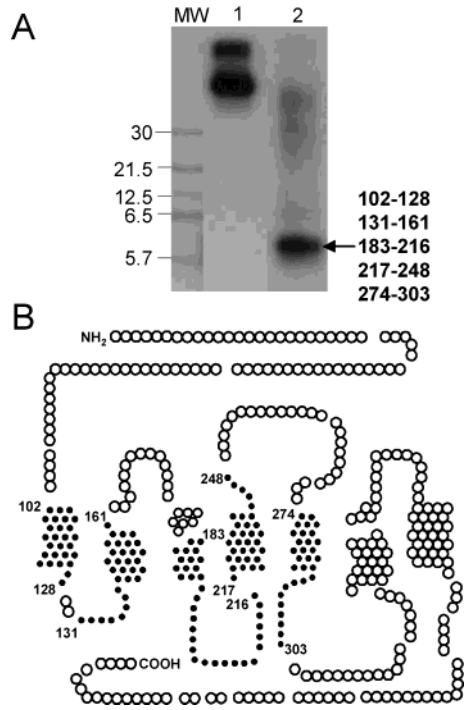

FIGURE 6: Endo Lys-C digestion of ET_B receptors photolabeled with [Bpa^5,$Tyr(^{125}I)^6$]IRL-1620. (A) Partially purified photolabeled ET_B receptors were incubated in the absence (lane 1) or in the presence of 1 μg Endo Lys-C (lane 2) at 37 °C for 18 h. All samples were run on a 16.5% acrylamide-tris-tricine separating gel followed by autoradiography. ^{14}C-Labeled protein standards of the indicated molecular masses (in kilodaltons) were run in parallel. These results are representative of at least three separate experiments. (B) Two-dimensional representation of the ET_B receptor shows five possible fragments in black closed circles bound to the photolabile ligand after the Endo Lys-C digestion.

the addition of 5 mM EDTA was shown to strongly reduce its presence (data not shown).

Analysis of Products of Proteolysis and Chemical Cleavage. To identify the binding domain, the ET_B receptor photolabeled with [Bpa^5,$Tyr(^{125}I)^6$]IRL-1620 was partially purified by SDS−PAGE and submitted to Endo Lys-C digestion, which cleaves on the C-terminal side of lysine residues. This enzymatic cleavage produced on a 16.5% acrylamide-tris-tricine separating gel, a well-resolved fragment at 5.9 kDa (lane 2 of Figure 6A) that would correspond to the smallest digestion fragment of the photolabeled receptor. Because the iodinated photoprobe has a mass of 2.1 kDa, the photolabeled segment would possess a molecular weight at around 3.8 kDa. According to the analysis of the primary structure of the ET_B receptor, five fragments could match these mass data, i.e., Tyr^{102}-Lys^{128} (3 kDa), Cys^{131}-Lys^{161} (3.4 kDa), Ala^{183}-Lys^{216} (3.5 kDa), Trp^{217}-Lys^{248} (3.6 kDa), and Asp^{274}-Lys^{303} (3.8 kDa) (Figure 6B).

To further define the labeled region, we proceeded to an alternative digestion step of the photolabeled [Bpa^5,$Tyr(^{125}I)^6$]-IRL-1620−ET_B complex with the V8 enzyme, which cleaves peptide bonds exclusively on the carboxylic side of aspartate and glutamate residues. Again, many bands are observed, thus suggesting an incomplete digestion (lane 1 of Figure 7A). Nevertheless, the analysis of the bands revealed that the shortest fragment exhibits a mass of 6.7 kDa corresponding to the sum of the photoprobe mass (2.1 kDa) and that of the photolabeled segment (4.6 kDa). A computerized analysis (with the Peptide Mass software) of the ET_B receptor

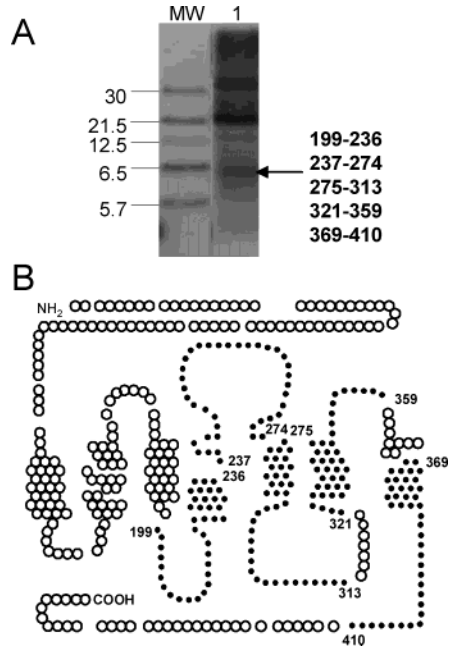

FIGURE 7: V8 protease digestion of ET_B receptors photolabeled with [Bpa^5,$Tyr(^{125}I)^6$]IRL-1620. (A) Partially purified photolabeled ET_B receptors were incubated in the presence of 8 μg V8 protease (lane 1) at room temperature for 7 days. The sample was run on a 16.5% acrylamide-tris-tricine separating gel followed by autoradiography. ^{14}C-Labeled protein standards of the indicated molecular masses (in kilodaltons) were run in parallel. These results are representative of at least three separate experiments. (B) Two-dimensional representation of the ET_B receptor shows five possible fragments in black closed circles bound to the photolabile ligand after the V8 protease digestion.

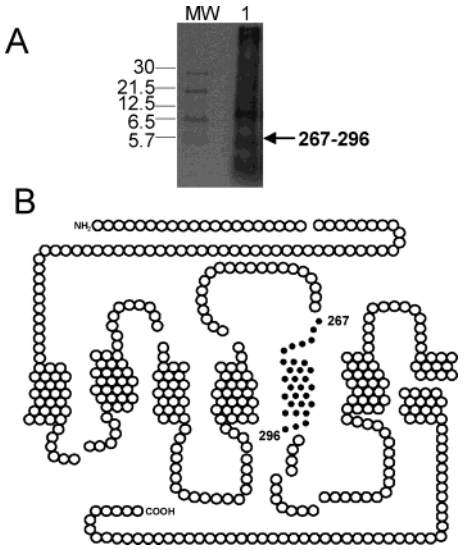

FIGURE 8: CNBr cleavage of ET_B receptors photolabeled with [Bpa^5,$Tyr(^{125}I)^6$]IRL-1620. (A) Partially purified photolabeled ET_B receptors were incubated in the presence of CNBr (125 mg/mL) (lane 1) at room temperature for 18 h in the dark. The sample was run on a 16.5% acrylamide-tris-tricine separating gel followed by autoradiography. ^{14}C-Labeled protein standards of the indicated molecular masses (in kilodaltons) were run in parallel. These results are representative of at least three separate experiments. (B) Two-dimensional representation of the ET_B receptor shows one possible fragment in black closed circles bound to the photolabile ligand after the CNBr cleavage.

sequence and of its fragments produced after complete and partial V8 digestion identified five peptide segments (Arg^{199}-Glu^{236}, Ala^{237}-Asp^{274}, Trp^{275}-Asp^{313}, Val^{321}-Glu^{359}, and Tyr^{369}-Glu^{410}) corresponding to a mass of 4.6 kDa. Except for the last suggestion, all four others would be produced after an incomplete digestion by the enzyme. As mentioned above and demonstrated by the number of bands of various molecular weights observed on the gel, even a prolonged V8 treatment (7 days) did not lead to a complete digestion. However, by combining the Endo Lys-C and V8 digestion results, we can reject the possibility that the last fragment Tyr^{369}-Glu^{410} is part of the binding domain because none of the expected proteolytic segments shows any overlaps. Taking into account that the labeled sequence produced by the two different enzymatic digestions must overlap, the V8 digestion fragment Val^{321}-Glu^{359} must also be rejected as the binding domain as well as the Endo Lys-C fragments Tyr^{102}-Lys^{128} and Cys^{131}-Lys^{161}. Therefore, the binding region would be located between Asp^{199}-Lys^{303}.

To further confirm the labeling site, we proceeded to a chemical treatment with CNBr that cleaves at the carboxylic side of methionine residues. Again, many bands are observed suggesting an incomplete digestion (lane 1 of Figure 8). Nevertheless, the analysis of the shortest fragment, appearing on the gel just before some residual free ligand, revealed a mass of 5.7 kDa that would be the sum of the photoprobe mass (2.1 kDa) and that of the photolabeled fragment (3.6 kDa). Moreover, the band appearing at around 8.4 kDa would correspond to the partially digested fragment Asp^{246}-Met^{296} linked to the photoprobe. On the basis of these SDS−PAGE results, only one segment, corresponding to Gln^{267}-Met^{296} (3.7 kDa) can fulfill the entire data.

DISCUSSION

The identification of the molecular determinants involved in the affinity of a ligand to its receptor is of utmost importance to understand the activation process. A few technologies are designed to reach this goal, and photoaffinity labeling appears as a useful strategy for exploring the binding area within a receptor. This approach relies on the affinity of a radioactive photoligand toward a receptor protein and on its ability to form a covalent conjugate that can be mapped subsequently. Hence, in the present study, we prepared five photosensitive probes exhibiting structures related to that of IRL-1620, a specific ET_B agonist.

A L-Bpa scanning was used for the development of specific photolabile probes for ET_B receptors. Thus, the photosensitive analogues were synthesized by substituting successively Ala^4, Val^5, Phe^7, His^9, and Leu^{10} with a Bpa residue. The other positions in the sequence were kept intact. Accordingly, as shown with structure−activity studies of IRL-1620 (*24*), it was established that N-succinoylation, peptide length, and the presence of a polyanionic cluster formed by the four carboxylic functions at the N terminus (Suc-Asp^1-Glu^2-Glu^3) were essential features to conserve the selectivity toward ET_B. For instance, the replacement of Asp^{11} with an uncharged amino acid such as Gly resulted in a 10-fold increase in affinity toward the ET_A receptor (*29*). Hence, these charged amino acids were not considered for Bpa swap. Similarly, the C-terminal residues Asp^{11}, Ile^{12}, Ile^{13}, and Trp^{14} were not substituted because structure−function analyses of ET confirmed their major roles in affinity (*30*, *31*). Finally, Tyr^6 in IRL-1620 was conserved because of the usefulness of this

residue for radiolabeling, whereas Ala was maintained in position 8 to preserve that key feature for the ET_B receptor. Indeed, in ET, it was described that substitution with Ala at positions Cys^3 and Cys^{11} did not have a large detrimental effect on the ET_A activity (2.3 versus 0.94 nM), but substitutions of Cys^1 and Cys^{15} extensively decreased the ET_A activity (170 versus 0.94 nM) without causing a very significant reduction of the ET_B effect (*32*). In IRL-1620, the template compound of the present study, residues matching Cys^1 and Cys^3 of ET are missing. However, in this derivative, the ET-corresponding Cys^{11} and Cys^{15} are substituted with Ala and Ala^{15} represents a crucial characteristic related to ET_B specificity. As a matter of fact, as described before by Saeki et al. (*33*), ET fragments with for instance alanine in position 15 exhibit a better affinity toward ET_B receptor preparations, as compared to their cysteine-containing counterparts.

All five photoprobes were characterized for their capacity to selectively recognize and activate the ET_B receptor. Biological activity studies showed that the amino acid residues Ala^4, Val^5, and Phe^7 are more tolerant to Bpa substitution than His^9 or Leu^{10}. This was somewhat surprising because previous ET studies showed that His^{16} (His^9 in IRL-1620) and Leu^{17} (Leu^{10} in IRL-1620) of ET-1 were not essential residues for binding and activity (*34*, *35*). Therefore, these results suggest that steric hindrance is probably responsible for the loss of activity and binding capacity of the last two peptides rather than the modification of the chemical character of the pharmacophore. Nevertheless, so far, three out of five photoprobes showed a significant potency in the guinea pig lung parenchyma assay.

Iodination of the Bpa analogues modulated their contractile properties without affecting their selectivity. Hence, it appeared that the addition of an iodine atom into the tyrosine side chain most likely contributed to structural restrictions within the binding domain of the ET_B receptor and changed the hydrophobic character of the phenolic moiety. Although, iodination of IRL-1620 did not significantly modify its potency, the ligation of an iodine atom in the Bpa^7 and Bpa^9 derivatives led to a complete loss of activity and binding capacity. In contrast, [Bpa^4,$Tyr(I)^6$]IRL-1620 and [Bpa^5,$Tyr(I)^6$]IRL-1620 became after iodination more potent than their counterpart, but this chemical modification influenced their efficacy. Besides the increase of hydrophobicity and reduction of molecular mobility produced by the incorporation of a meta-iodine atom, a decrease of the phenolic pK_a of Tyr^6, coming from the electron-withdrawing effect of the halogen, might also be at the origin of those observations.

Among the synthetic photoprobes, both [Bpa^4,$Tyr(I)^6$]IRL-1620 and [Bpa^5,$Tyr(I)^6$]IRL-1620 kept their selective activity toward the guinea pig ET_B receptor. Competition binding experiments between [Bpa^5,$Tyr(^{125}I)^6$]IRL-1620 and unlabeled ET-1 or IRL-1620 showed that ET-1 is a better competitor than IRL-1620. In fact, when using [$Tyr(^{125}I)^6$]-IRL-1620 as a tracer, ET-1 appeared 2.3 times more potent than IRL-1620 for displacing the radioiodinated probe from the ET_B receptors expressed in CHO cells. In this study, with [Bpa^5,$Tyr(^{125}I)^6$]IRL-1620 as a radioactive probe, the potency of competition of ET-1 over IRL-1620 exhibited a 30-fold increase. On the other hand, competitive assays with this time [Bpa^4,$Tyr(^{125}I)^6$]IRL-1620 revealed a very weak binding capacity of this compound for the human ET_B receptors found in the CHO cells. It is known that IRL-1620 possesses different species-binding characteristics. For instance, in rat cerebellum, the binding is irreversible, while being reversible in other tissues such as the dog cerebellum and the human lung (*36*). Such different binding characteristics related to variations in the receptor sequence between species could explain why the [Bpa^4,$Tyr(I)^6$]IRL-1620 probe, while active in the guinea pig lung parenchyma, exhibited no binding capacity for the cloned human ET_B receptor.

Because photolabeling experiments were performed on human ET_B receptors tranfected in CHO cells, [Bpa^5]IRL-1620 was the only photoprobe used. This peptide specifically labeled the ET_B receptor, which migrated as two nonglycosylated entities, one with a mass of 49 kDa and another with a mass of 37 kDa. This particular observation was also made by Takasuka et al. (*19*) who reported that in the presence of 1% SDS, at reduced temperature, the [$Tyr(^{125}I)^{13}$]ET-1−ET_B receptor complex was stable but displayed, on SDS−PAGE analysis, two bands at approximate molecular weights of 50 and 35 kDa. The 49-kDa band that we obtained, corresponding to a complex formed by a protein attached covalently to [Bpa^5,$Tyr(^{125}I)^6$]IRL-1620, was shown to be superimposable to an ET_B receptor band identified by immunoblotting assays, using anti-ET_B polyclonal antibodies. Moreover, excess of ET-1 or IRL-1620 abolished the photolabeling of these two bands, demonstrating that [Bpa^5,$Tyr(^{125}I)^6$]IRL-1620 competes for the same binding site. Our data are as well in agreement with other characterization studies of the ET_B receptor as those performed after cross-linking [$Tyr(^{125}I)^{13}$]-ET-1 to the receptor using the bifunctional reagents disuccinimidyl suberate, bis(sulfosuccinimidyl)suberate, or *N*-hydroxysuccinimidyl-4-azidobenzoate (*37*−*40*). Furthermore, as described in a recent report by Grantcharova et al. (*41*), the 37-kDa protein would be the N-terminally truncated receptor produced by the action of a metalloprotease. Thus, the N-terminal segment of the ET_B receptor would be cleaved following a limited proteolysis between residues Arg^{64} and Ser^{65}. This result provides interesting data on the binding site of [Bpa^5,$Tyr(^{125}I)^6$]IRL-1620 because it shows that the interaction of this specific radiolabeled photoprobe would not be within the 1−64 segment of the ET_B receptor. Interestingly, addition of 5 mM EDTA during photolabeling allowed a better recovery of the full-length ET_B receptor because the proteolysis was considerably diminished.

To better define the binding site of [Bpa^5,$Tyr(^{125}I)^6$]IRL-1620 on ET_B receptors, the photolabeled complex was cleaved using either Endo Lys-C protease, V8 protease, or CNBr. According to the selectivity of these enzymatic or chemical treatments and considering that radiolabeled fragments produced by them must overlap, the 3.8-kDa segment formed after Endo Lys-C treatment would be composed of residues Asp^{274}-Lys^{303}, the 4.6-kDa fragment of V8 protease would be composed of residues Trp^{275}-Asp^{313}, and CNBr would have produced the fragment Gln^{267}-Met^{296} with a mass of 3.7 kDa. When taken together, these data clearly identify a common sequence of 2.8 kDa that would correspond to residues Trp^{275}-Met^{296} (Figure 9). In other words, this cell-surface-oriented segment of the fifth TM domain of the ET_B receptor would play an important role in the binding of the photoprobe [Bpa^5,$Tyr(^{125}I)^6$]IRL-1620. These results are in agreement with data obtained by Sakamoto and co-workers with a series of ET_A and ET_B receptor chimeras. Actually,

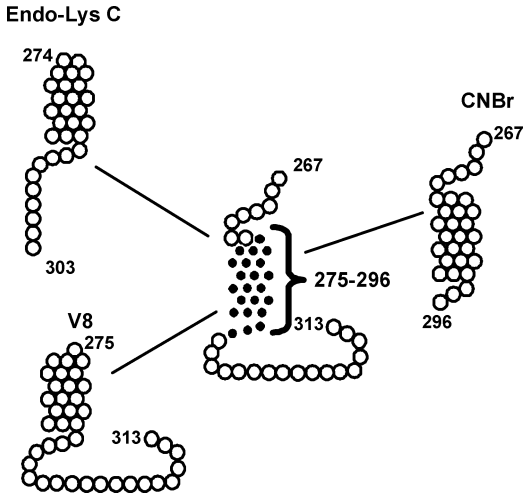

FIGURE 9: Schematic representation of the labeled domain of the ET_B receptor after covalent bonding with [Bpa^5,Tyr(^{125}I)^6]IRL-1620. According to CNBr cleavage and Endo Lys-C and V8 protease digestions, receptor residues 275−296 form the common fragment between all of the cleaved photolabeled fragments.

they demonstrated that an ET_A−ET_B receptor hybrid obtained by replacing the TM helices IV, V, and VI of ET_A with those from ET_B can then bind IRL-1620 (*18*).

Finally, the observation that an excess of ET-1 and IRL-1620 abolished the photolabeling of the ET_B receptor produced with [Bpa^5,Tyr(^{125}I)^6]IRL-1620 suggests that all of these peptides share the same binding site that would contain, according to our data, the Trp^{275}-Met^{296} stretch. Moreover, after the demonstration by Imumara et al. that the mutation of Trp^{276} to Cys and Trp^{275} to Ala, within the hET_B receptor, did not give rise to any modifications of affinity toward ET-1 and IRL-1620 (*42*), it can be presumed that the two tryptophan residues would not be involved in the direct binding to the ligand, thus suggesting that the affinity domain of ET_B for [Bpa^5,Tyr(^{125}I)^6]IRL-1620 would be within the Leu^{277}-Met^{296} segment.

In conclusion, using the photoaffinity-labeling technique, we identify a key segment of the ET_B receptor participating in the interaction with the ET-1 of IRL-1620 ligands. This protocol had the advantage that an unaltered form of the receptor, as obtained for instance with the site-directed mutagenesis technique, was explored. Further structural and binding data will however be required to complete molecular dissection of the ET_B-binding pocket. This study is thus pursued using this time photoprobes derived from specific ET_B antagonists.

ACKNOWLEDGMENT

The authors thank Myriam Létourneau, Chantal Langlois, Steve Bourgault, and Alexandra Louimaire for their assistance and proofreading.

REFERENCES

1. Yanagisawa, M., Kurihara, H., Kimura, S., Tomobe, Y., Kobayashi, M., Mitsui, Y., Yazaki, Y., Goto, K., and Masaki, T. (1988) A novel potent vasoconstrictor peptide produced by vascular endothelial cells, *Nature 332*, 411−415.
2. Inoue, A., Yanagisawa, M., Kimura, S., Kasuya, Y., Miyauchi, T., Goto, K., and Masaki, T. (1989) The human endothelin family: Three structurally and pharmacologically distinct isopeptides predicted by three separate genes, *Proc. Natl. Acad. Sci. U.S.A. 86*, 2863−2867.
3. Goraca, A. (2002) New views on the role of endothelin, *Endocr. Regul. 36*, 161−167.
4. Touyz, R. M., and Schiffrin, E. L. (2003) Role of endothelin in human hypertension, *Can. J. Physiol. Pharmacol. 81*, 533−541.
5. Orth, S. R., Viedt, C., Amann, K., and Ritz, E. (2001) Endothelin in renal diseases and cardiovascular remodeling in renal failure, *Intern. Med. 40*, 285−291.
6. Schmitz-Spanke, S., and Schipke, J. D. (2000) Potential role of endothelin-1 and endothelin antagonists in cardiovascular diseases, *Basic Res. Cardiol. 95*, 290−298.
7. Masaki, T., Vane, J. R., and Vanhoutte, P. M. (1994) International Union of Pharmacology nomenclature of endothelin receptors, *Pharmacol. Rev. 46*, 137−142.
8. Shetty, S. S., Okada, T., Webb, R. L., DelGrande, D., and Lappe, R. W. (1993) Functionally distinct endothelin B receptors in vascular endothelium and smooth muscle, *Biochem. Biophys. Res. Commun. 191*, 459−464.
9. Masaki, T., Ninomiya, H., Sakamoto, A., and Okamoto, Y., (1999) Structural basis of the function of endothelin receptor, *Mol. Cell. Biochem. 190*, 153−156.
10. Breu, V., Hashido, K., Broger, C., Miyamoto, C., Furuichi, Y., Hayes, A., Kalina, B., Loffler, B. M., Ramuz, H., and Clozel, M. (1995) Separable binding sites for the natural agonist endothelin-1 and the non-peptide antagonist bosentan on human endothelin-A receptors, *Eur. J. Biochem. 231*, 266−270.
11. Wada, K., Hashido, K., Terashima, H., Adachi, M., Fujii, Y., Hiraoka, O., Furuichi, Y., and Miyamoto, C. (1995) Ligand binding domain of the human endothelin-B subtype receptor, *Protein Expression Purif. 6*, 228−236.
12. Mosberg, H. I., and Fowler, C. B. (2002) Development and validation of opioid ligand−receptor interaction models: The structural basis of μ vs. δ selectivity, *J. Pept. Res. 60*, 329−335.
13. Iwashina, M., Mizuno, T., Hirose, S., Ito, T., and Hagiwara, H. (1994) His^{145}-Trp^{146} residues and the disulfide-linked loops in atrial natriuretic peptide receptor are critical for the ligand-binding activity, *J. Biochem. 115*, 563−567.
14. Rose, P. M., Krystek, S. R., Jr., Patel, P. S., Liu, E. C., Lynch, J. S., Lach, D. A., Fisher, S. M., and Webb, M. L. (1995) Aspartate mutation distinguishes ET_A but not ET_B receptor subtype-selective ligand binding while abolishing phospholipase C activation in both receptors, *FEBS Lett. 361*, 243−249.
15. Fukuoka, Y., Ember, J. A., and Hugli, T. E. (1999) Ligand binding sites on guinea-pig C3aR: Point and deletion mutations in the large extracellular loop and vicinity, *Biochem. Biophys. Res. Commun. 263*, 357−360.
16. Zhu, G., Wu, L. H., Mauzy, C., Egloff, A. M., Mirzadegan, T., and Chung, F. Z. (1992) Replacement of lysine-181 by aspartic acid in the third transmembrane region of endothelin type B receptor reduces its affinity to endothelin peptides and sarafotoxin 6c without affecting G protein coupling, *J. Cell. Biochem. 50*, 159−164.
17. Adachi, M., Furuichi, Y., and Miyamoto, C. (1994) Identification of specific regions of the human endothelin-B receptor required for high affinity binding with endothelin-3, *Biochim. Biophys. Acta 1223*, 202−208.
18. Sakamoto, A., Yanagisawa, M., Sawamura, T., Enoki, T., Ohtani, T., Sakurai, T., Nakao, K., Toyo-oka, T., and Masaki, T. (1993) Distinct subdomains of human endothelin receptors determine their selectivity to endothelinA-selective antagonist and endothelinB-selective agonists, *J. Biol. Chem. 268*, 8547−8553.
19. Takasuka, T., Sakurai, T., Goto, K., Furuichi, Y., and Watanabe, T. (1994) Human endothelin receptor ET_B. Amino acid sequence requirements for super stable complex formation with its ligand, *J. Biol. Chem. 269*, 7509−7513.
20. Kauer, J. C., Erickson-Viitanen, S., Wolfe, H. R., Jr., and DeGrado, W. F. (1986) *p*-Benzoyl-L-phenylalanine, a new photoreactive amino acid. Photolabeling of calmodulin with a synthetic calmodulin-binding peptide, *J. Biol. Chem. 261*, 10695−10700.
21. Bremer, A. A., Leeman, S. E., and Boyd, N. D. (2001) Evidence for spatial proximity of two distinct receptor regions in the substance P (SP)*neurokinin-1 receptor (NK-1R) complex obtained by photolabeling the NK-1R with *p*-benzoylphenylalanine3-SP, *J. Biol. Chem. 276*, 22857−22861.
22. Pérodin, J., Deraet, M., Auger-Messier, M., Boucard, A. A., Rihakova, L., Beaulieu, M.-E., Lavigne, P., Parent, J.-L., Guillemette, G., Leduc R., and Escher, E. (2002) Residues 293 and 294 are ligand contact points of the human angiotensin type 1 receptor, *Biochemistry 41*, 14348−14356.

23. Boucard, A. A., Sauvé, S. S., Guillemette, G., Escher, E., and Leduc, R. (2003) Photolabelling the rat urotensin II/GPR14 receptor identifies a ligand-binding site in the fourth transmembrane domain, *Biochem. J. 370*, 829−838.
24. Takai, M., Umemura, I., Yamasaki, K., Watakabe, T., Fujitani, Y., Oda, K., Urade, Y., Inui, T., Yamamura, T., and Okada, T. (1992) A potent and specific agonist, Suc-[Glu^9,$Ala^{11,15}$]-endothelin-1(8−21), IRL 1620, for the ET_B receptor, *Biochem. Biophys. Res. Commun. 184*, 953−959.
25. Watakabe, T., Urade, Y., Takai, M., Umemura, I., and Okada, T. (1992) A reversible radioligand specific for the ET_B receptor, *Biochem. Biophys. Res. Commun. 185*, 867−873.
26. Nguyen, P. V., Yang, X. P., Li, G., Deng, L. Y., Fluckiger, J. P., and Schiffrin, E. L. (1993) Contractile responses and signal transduction of endothelin-1 in aorta and mesenteric vasculature of adult spontaneously hypertensive rats, *Can. J. Physiol. Pharmacol. 71*, 473−483.
27. Wong, W.-S. F., Bloomquist, S. L., Bendele, A. M., and Fleisch, J. H. (1992) Pharmacological and histological examinations of regional differences of guinea-pig lung: A role of pleural surface smooth muscle in lung strip contraction, *Br. J. Pharmacol. 105*, 620−626.
28. Laemmli, U. K. (1970) Cleavage of structural proteins during the assembly of the head of bacteriophage T4, *Nature 227*, 680−685.
29. Katahira, R., Umemura, I., Takai, M., Oda, K., Okada, T., and Nosaka, A. Y. (1998) Structural studies on endothelin receptor subtype B specific agonist IRL 1620, *J. Pept. Res. 51*, 155−164.
30. Rovero, P., Galoppini, C., Laricchia-Robbio, L., Mazzoni, M. R., and Revoltella, R. P. (1998) Structure−activity analysis of C-terminal endothelin analogues, *J. Cardiovasc. Pharmacol. 31* (Suppl. 1), S251−S254.
31. Cassano, E., Galoppini, C., Giusti, L., Hamdan, M., Macchia, M., Mazzoni, M. R., Menchini, E., Pegoraro, S., and Rovero, P. (1998) A structure−activity study of a C-terminal endothelin analogue, *Folia Biol. 44* (1), 11−14.
32. Topouzis, S., Huggins, J. P., Pelton, J. T., and Miller, R. C. (1991) Modulation by endothelium of the responses induced by endothelin-1 and by some of its analogues in rat isolated aorta, *Br. J. Pharmacol. 102*, 545−549.
33. Saeki, T., Ihara, M., Fukuroda, T., Yamagiwa, M., and Yano, M. (1991) [$Ala^{1,3,11,15}$]-Endothelin-1 analogs with ET_B agonist activity, *Biochem. Biophys. Res. Commun. 179*, 286−292.
34. Forget, M.-A., Lebel, N., Sirois, P., Boulanger, Y., and Fournier, A. (1996) Biological and molecular analyses of structurally reduced analogues of endothelin-1, *Mol. Pharmacol. 49*, 1071−1079.
35. Tam, J. P., Liu, W., Zhang, J.-W., Galantiro, M., Bertolero, F., Cristiani, C., Vaghi, F., and Castiglione, R. (1994) Alanine scan of endothelin: Importance of aromatic residues, *Peptides 15*, 703−708.
36. Nambi, P., Pullen, M., and Spielman, W. (1994) Species differences in the binding characteristics of [^{125}I]IRL-1620, a potent agonist specific for endothelin-B receptors, *J. Pharmacol. Exp. Ther. 268*, 202−207.
37. Miyazaki, H., Kondoh, M., Watanabe, H., Masuda, Y., Murakami, K., Takahashi, M., Yanagisawa, M., Kimura, S., Goto, K., and Masaki, T. (1990) Affinity labelling of endothelin receptor and characterization of solubilized endothelin-endothelin-receptor complex, *Eur. J. Biochem. 187*, 125−129.
38. Schvartz, I., Ittoop, O., and Hazum, E. (1990) Identification of endothelin receptors by chemical cross-linking, *Endocrinology 126*, 1829−1833.
39. Chiou, W. J., Magnuson, S. R., Dixon, D., Sundy, S., Opgenorth, T. J., and Wu-Wong, J. R. (1997) Dissociation characteristics of endothelin receptor agonists and antagonists in cloned human type-B endothelin receptor, *Endothelium 5*, 179−189.
40. Nambi, P., Pullen, M., Kincaid, J., Nuthulaganti, P., Aiyar, N., Brooks, D. P., Gellai, M., and Kumar, C. (1997) Identification and characterization of a novel endothelin receptor that binds both ET_A- and ET_B-selective ligands, *Mol. Pharmacol. 52*, 582−589.
41. Grantcharova, E., Furkert, J., Reusch, H. P., Krell, H. W., Papsdorf, G., Beyermann, M., Schulein, R., Rosenthal, W., and Oksche, A. (2002) The extracellular N terminus of the endothelin B (ET_B) receptor is cleaved by a metalloprotease in an agonist-dependent process, *J. Biol. Chem. 277*, 43933−43941.
42. Imumara, F., Arimoto, I., Fujiyoshi, Y., and Doi, T. (2000) W276 mutation in the endothelin receptor subtype B impairs Gq coupling but not Gi or Go coupling, *Biochemistry 39*, 686−692.

BI049246X